Journal of Applied Physics

RESEARCH ARTICLE | MAY 17 2024

Imaging spatial plasmon mode of nanocavity formed by Au tip and Au nanorod lattice in tip-enhanced Raman spectroscopy

Zhe He ; Jue Wang ; Rui Wang ; Dmitry Kurouski

J. Appl. Phys. 135, 193110 (2024)
https://doi.org/10.1063/5.0199473

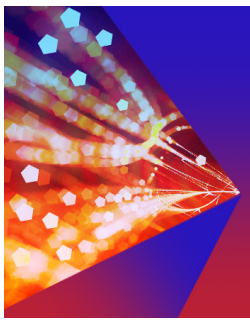

Journal of Applied Physics ARTICLE pubs.aip.org/aip/jap

Imaging spatial plasmon mode of nanocavity formed by Au tip and Au nanorod lattice in tip-enhanced Raman spectroscopy

Cite as: J. Appl. Phys. **135**, 193110 (2024); doi: 10.1063/5.0199473
Submitted: 19 February 2024 · Accepted: 5 May 2024 ·
Published Online: 17 May 2024

Zhe He,[1] Jue Wang,[2] Rui Wang,[2,3,a)] and Dmitry Kurouski[3,4,a)]

AFFILIATIONS

[1]Shandong Institute of Advanced Technology, Jinan, Shandong, China
[2]State Key Laboratory of Digital Medical Engineering, School of Biological Science & Medical Engineering, Southeast University, Nanjing, Jiangsu, China
[3]Department of Biochemistry and Biophysics, Texas A&M University, College Station, Texas 77843, USA
[4]The Institute for Quantum Science and Engineering, Texas A&M University, College Station, Texas 77843, USA

[a)]**Author to whom correspondence should be addressed:** dkurouski@tamu.edu

ABSTRACT

The integration of Au nanorods in tip-enhanced Raman spectroscopy (TERS) presents a significant increase in the enhancement factor, primarily due to the gap-mode effect. By aligning Au nanorods in parallel, we construct an Au nanorod lattice, referred to as the Au nanolattice, which further amplifies the advantages of TERS imaging due to the induced inter-nanorod surface plasmon resonance. A critical aspect in this research involves investigating the distribution of hotspots within the nanolattice during TERS measurements. Additionally, we demonstrate that the tip–lattice nanocavity is a predominant factor in determining both the intensity and spatial distribution of these hotspots. Employing the experimental and simulation results, we illustrate the enhancement effect of the tip–lattice cavity and elucidate the connection between the hotspot intensity and cavity size. This comprehensive approach contributes to our understanding of the nanolattice's role in TERS and offers valuable insights for optimizing nanophotonic applications.

INTRODUCTION

Metallic nanorods, characterized by their surface plasmon resonance (SPR), have emerged as versatile platforms with extraordinary optical properties.[1–3] SPR plays a predominant role in various applications, particularly in surface-enhanced Raman spectroscopy (SERS)[4,5] and single-molecule photocatalysis.[6,7] The unique electronic properties of Au nanorods make them ideal candidates for enhancing Raman signal sensitivity and facilitating photocatalysis at the single-molecule level. In contrast to individual Au nanorod, the nanorod lattice (i.e., self-assemblies of individual nanorods) offers unique advantages, providing collective behavior that transcends the characteristics of individual nanorod.[8,9] This ordered assemble enhances the overall optical and electronic properties, facilitating advanced applications in sensing and photocatalysis.[10]

A key feature of the nanorod lattice is its collective plasmon mode, resulting from interactions among adjacent nanorods.[11] This collective plasmon mode leads to tunable and enhanced plasmonic responses; thus, imaging spatial plasmon modes provides information regarding the SPR mode and its distribution, which is crucial for developing cutting-edge nanophotonic devices and applications. Up to now, the experimental measurement of nanorod plasmon modes has been accomplished through a variety of advanced techniques like dark-field microscopy[12,13] and scattering-type scanning near-field optical microscopy (s-SNOM),[14] which provides spatially resolved information on plasmonic excitations. Additionally, electron energy-loss spectroscopy (EELS) in transmission electron microscopy (TEM) has enabled detailed investigations into the energy and spatial distribution of plasmon resonances.[15,16] However, investigating plasmon modes in the nanorod lattice remains challenging, primarily owing to the ultrasmall dimensions (down to a few nanometers) of nanocavities formed within these lattices.[17] Although TEM can image sub-nanometer structures,

in situ detection of plasmon modes is still limited. Therefore, it is highly desired to develop an imaging technique, which is capable of *in situ* imaging plasmon modes of nanorod lattice at nanoscale.

Tip-enhanced Raman spectroscopy (TERS) stands as a powerful technique for mapping intricate plasmon modes within structures like the Au nanorod lattice.[18] TERS employs a metallic tip (such as Au tip) in close proximity to the sample, thereby amplifying the Raman signal and achieving nanoscale spatial resolution. Specifically, the tip forms a plasmon cavity with the nanolattice, enhancing the SPR through the gap-mode effect.[19] Therefore, both the materials of the tip and nanolattice influence the enhancement factor.[20] With enhanced SPR, a detection limit down to single molecules and nanometer-sized spatial resolution can be achieved, which is crucial for imaging the hotspots' distribution in the Au nanolattice.

In this work, we adopted a single mono-layer of p-nitrothiophenol (pNTP) molecules on the nanolattice as transducer molecules.[18] The Raman band of nitro group (1330 cm^{-1}) imaged by TERS indicates the hotspot positions within the nanolattice. Notably, the uniform single monolayer ensures unbiased hotspot measurements, allowing us to pinpoint the regions of the heightened plasmonic activity and gain insights into the spatial distribution of plasmon resonances. Through precise characterization of plasmon hotspots, we can fabricate nanolattices to achieve specific optical responses. Moreover, experimentally mapping plasmon modes is essential for unlocking the full potential of Au nanorod lattices in nanophotonic and nanocatalytic applications. Finally, we utilize the synergy between experimental and simulation validation to propel the optimization of nanolattices for TERS.

RESULTS

The hotspots on the Au nanorod predominantly manifest at their longitudinal ends based on the Localized surface plasmon resonances (LSPR) mode of a single nanorod. In the case of an 80 nm-long nanorod, higher-order plasmon modes are less conspicuous.[18,21] Consequently, utilizing nanorods as a TERS substrate for applications such as single-molecule sensing allows for the measurement of doped molecules in a relatively confined region.[22] Figure 1 provides a numerical simulation illustrating this phenomenon, where exciting the nanorods along the longitudinal direction generates a well-defined plasmon mode, offering valuable insights for optimizing TERS applications and nanorod behavior. The absorption spectrum of the Au nanorods is presented in Fig. S2 in the supplementary material.

As shown in Fig. 1, placing an Au tip with a radius of 20 nm and length of 80 nm above the nanorods creates a nano-cavity, intensifying the electric field of the hotspot. This enhancement results from the coupling of the plasmon modes of the nanorods with that of the tip. Regions with higher plasmon density improve field enhancements for the nano-cavity. Simultaneously, the tip can alter the intrinsic plasmon mode of the nanorods. We utilize TERS to image the doped pNTP monolayer that uniformly covers the whole nanolattice, effectively mapping the hotspots within the tip–lattice gap-mode plasmonic structure.

Through the parallel alignment of multiple nanorods,[23] we have successfully engineered a nanolattice, as depicted by AFM image [Fig. 2(a)] and SEM image (Fig. S1 in the Supplementary Material).

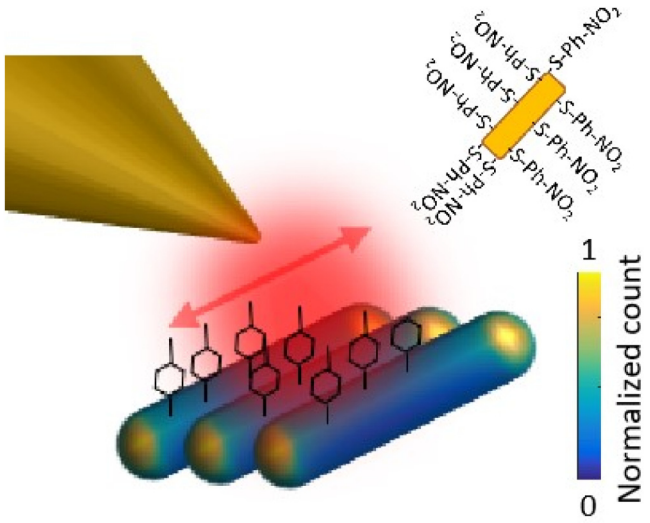

FIG. 1. Schematics of TERS in conjunction with an Au nanorod lattice. The red arrow represents the polarization direction of the incidence light. The nanorods are uniformly covered with a monolayer of pNTP molecules. In this configuration, the tip-nanorod-lattice cavity is shown to enhance the Raman signal of the nitro group ($-NO_2$), which maps the positions of the hotspots. Numerical simulations reveal that the hotspots are located at the ends of each nanorod under the given polarization condition.

The scale bar in Fig. 2(a) characterizes the nanorod diameter, approximately 20 nm. Notably, the right part appears thicker due to the overlap of two nanorods. When the lattice aligns perpendicular to the light polarization, hotspots are anticipated to manifest at the two ends of each nanorod. However, as illustrated in Fig. 2(b), the observed plasmon modes between nanorods emerge due to the lattice structure. In the specified area, the enhancement effect covers the entire nanorods, particularly accentuating hotspots at the midpoint. Figure 2(c) presents a typical TERS spectrum of pNTP doped on the lattice, with the highlighted peak attributed to the nitro band, situated approximately 0.5 nm above the nanorods.[20] Note that the peak at 1391 cm^{-1} indicates a few $-NO_2$ is transformed to azo bonds, which suggests that photocatalysis occurs during imaging. However, as shown in Fig. S3 in the supplementary material, the sites generating azo are very sparse, affirming that the majority of TERS images remain unaffected by such chemical transformations.

As depicted in Fig. 3(a), when the dual-nanorod-lattice structure is selectively stimulated by polarized light aligned with its orientation, the lattice mode is generated. This selective stimulation emphasizes the lattice's unique plasmonic behavior. Figure 3(b) reveals the hotspots through imaging the enhancement of the nitro peak. Notably, compared to their central regions, the longitudinal ends of the nanorods exhibit subdued brightness.

To corroborate the experimental findings, simulations employing MNPBEM algorithms were conducted to illustrate the near-field intensity.[24] Figures 3(c)–3(f) show the simulated field intensities corresponding to different positions of the tip, varying

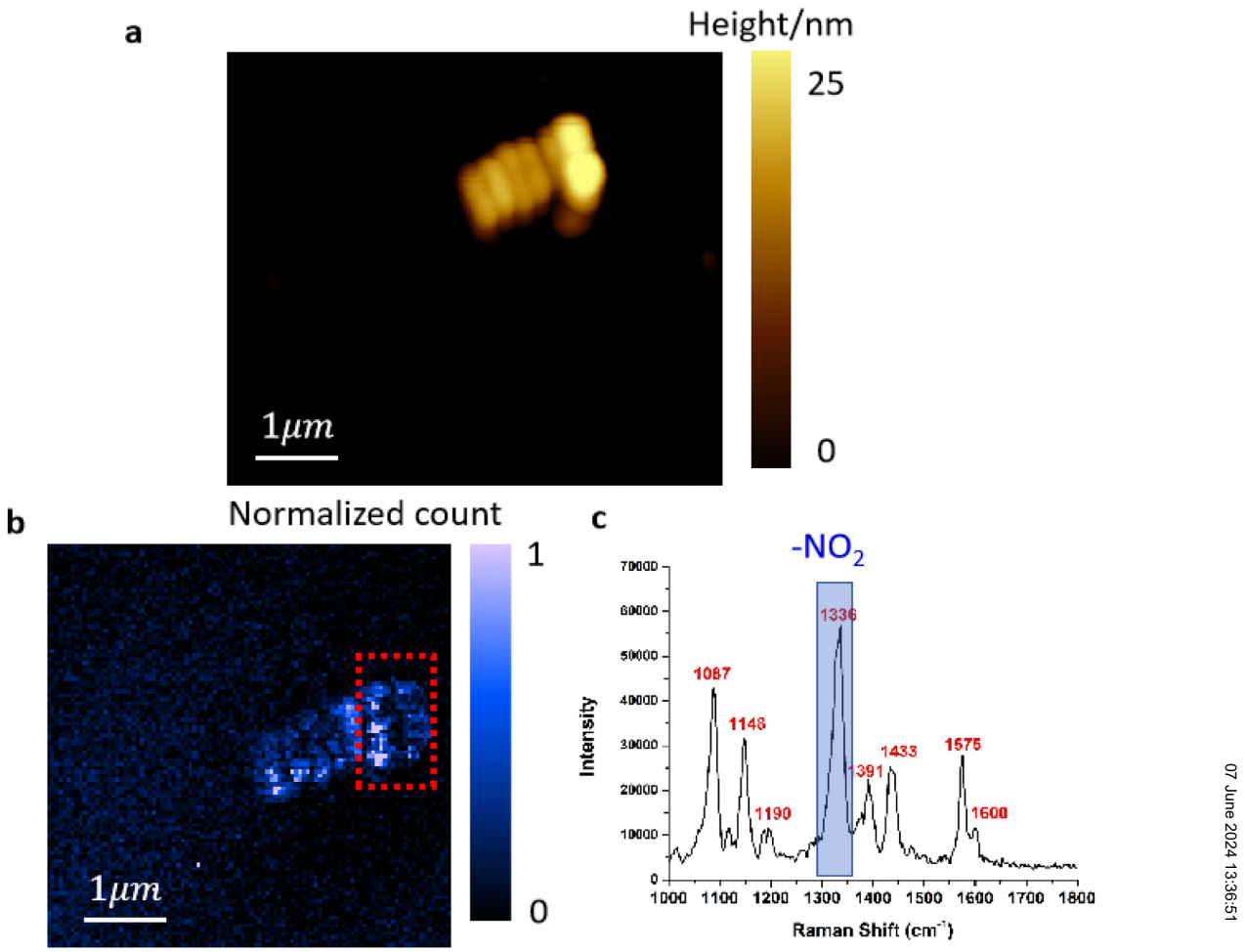

FIG. 2. TERS image of a nanorod lattice composed of 7 nanorods. (a), AFM image of the lattice. The radius of the nanorod is 20 nm, and the length is 80 nm. The right part of the selected structure is a dislocated stack of two nanorods, reaching a height of 25 nm. (b), TERS image of the same lattice. The color bar stands for the integrated intensity of the Raman peak 1336 cm^{-1}. The rectangular area shows the stacked nanorods. (c), the TERS spectrum of the pNTP layer on the nanolattice. The shaded peak is corresponding to -NO_2.

from being in contact with the nanolattice to retracting from it. Specifically, the gaps between the tip and the nanolattice were set at 0.1, 0.3, 0.5, and 0.7 nm, respectively. Notably, these simulations replicate the TERS measurement process rather than directly simulating the near-field plasmon mode. Throughout the measurement process, the tip traverses across the nanolattice. Therefore, we simulate the hotspot for each point of the scan. The assumption here is that the detector is positioned in the far field. Initially, the far-field electric intensity is computed using the nanolattice alone. Subsequently, a nanoparticle-like tip with a diameter of 20 nm is brought into contact with the nanolattice, and the resulting enhanced intensity is calculated. Finally, the difference between these two intensities yields the true near-field intensity. The spacing between the nanorods is fixed at 1 nm in Fig. 3, and its dependency is illustrated in Fig. S4 in the supplementary material.

At a tip position of 0.1 nm above the nanolattice, the simulation shows nearly uniform hotspots across both nanorods in TERS, resulting in a near-field intensity lower than that observed for gaps of 0.3 and 0.5 nm. Figure 3(e) illustrates that as the gap distance increases to 0.5 nm, in concordance with Fig. 3(b), the simulation demonstrates higher enhancement at the center of both nanorods, with comparatively weak hotspots at the longitudinal ends of the left nanorod. With the tip positioned 0.7 nm above the nanolattice, as depicted in Fig. 3(f), hotspots are primarily influenced by each nanorod, with the inter-nanorod plasmon making a weaker contribution. Simultaneously, the near-field enhancement is reduced. The simulations indicate that the plasmon modes of the nanolattice dominate the near-field enhancement when the tip-nanolattice gap is less than 0.7 nm.

The precise positioning of the tip above the nanolattice is of significance, particularly considering the thickness of the molecular

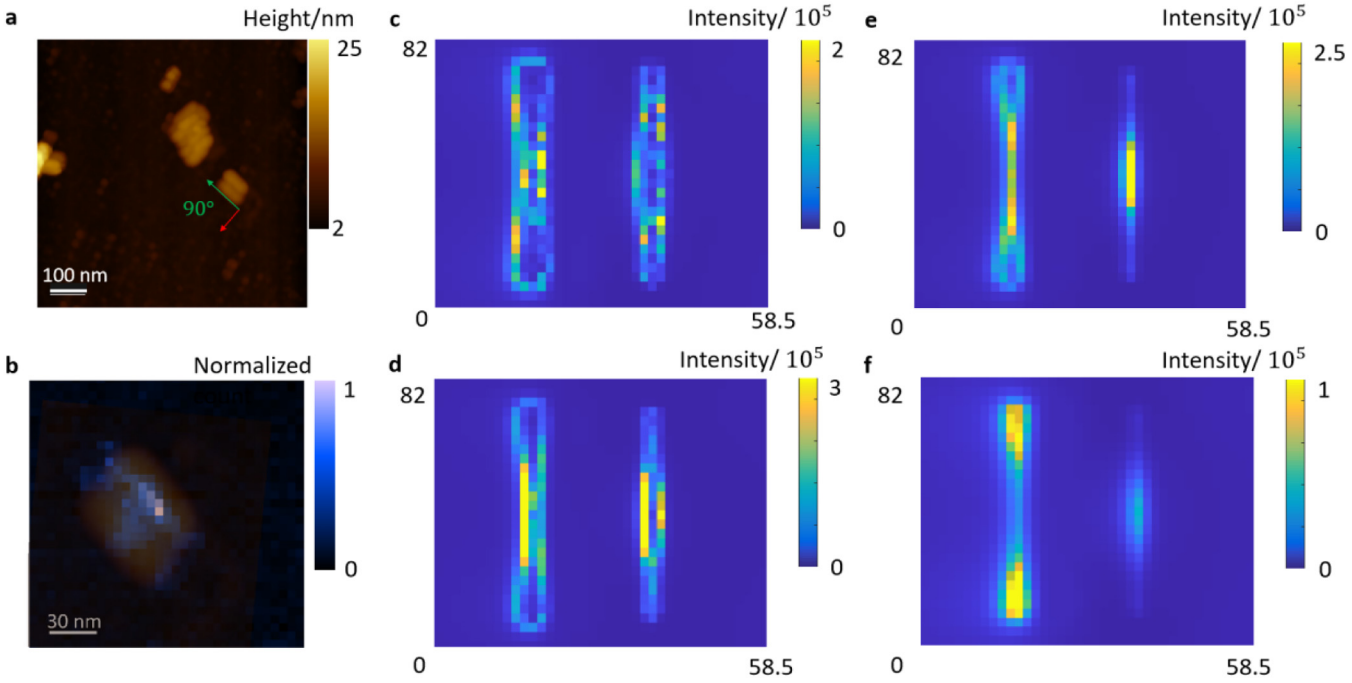

FIG. 3. TERS image and simulation of a dual-nanorod lattice. (a) AFM image of the dual-nanorod structure located on the right side of the image. The two nanorods are aligned parallel to each other. The polarization of the incident light is along the x-axis (indicated by the red arrow), making an angle of 90 degrees with the longitudinal axis of the nanorods. (b) the TERS image of the plasmon mode of the dual-nanorod structure. The AFM and TERS images are collocated to highlight the hotspot positions within the structure. (c)–(f) numerical simulations corresponding to the TERS image (b) showing the electric field intensity at various heights above the nanorods: (c) 0.1, (d) 0.3, (e) 0.5, (f) 0.7 nm. The axis unit is nm.

layer. For instance, to achieve optimal results, the tip is often positioned approximately 0.5 nm above the nanolattice. This distance is notably associated with the nitro band. It's noteworthy that the hotspots generated by the tip–lattice structure exhibit variability, depending on the specific cross-sectional plane under investigation. Therefore, careful consideration of these spatial parameters is important for effectively probing and understanding the intricate interactions within the nanolattice during experiments.

DISCUSSION

The hotspots generated by individual nanorods exhibit limited strength due to their low plasmon density. In contrast, hotspots induced by the lattice configuration manifest much larger intensity than those arising from individual nanorods. Furthermore, the distribution of these hotspots is demonstrated to be more expansive and uniform, offering significant advantages for two-dimensional single-molecule imaging. This observation underscores the distinct plasmonic properties of the dual-nanorod lattice, where the enhanced area displays a more uniform distribution of hotspots compared to individual nanorods. Smaller hotspots, typical of individual nanorods, result in speckled images, rendering them more aptly utilized in sensing applications without spatial resolution.

Traditionally, the investigation of hotspots in TERS has been linked to the plasmon mode of substrate structures. However, it is crucial to note that the near-field signal in TERS is not exclusively determined by the nanolattice; rather, the contribution of the tip–lattice nanocavity should be taken into account. As illustrated in Figs. 3(c)–3(f), the gap between the tip and the nanolattice plays a significant role in influencing hotspot distribution. Notably, for the pNTP molecule with its nitro band positioned approximately 0.5 nm above the nanolattice, Figs. 3(c) and 3(f) fail to accurately depict what is observed in Fig. 3(b). This underscores the importance of considering the specific interactions within the tip–lattice nanocavity for a comprehensive understanding of hotspot dynamics in TERS. As a reference, the simulation of a tip-rod cavity is demonstrated in Fig. S5 in the supplementary material. The further study of the dependence of the tip sizes is shown in Fig. S6 in the supplementary material.

The complexity of hotspot formation within the nanolattice surpasses that of a single nanorod due to its collective plasmonic effect, resulting in generally stronger enhancements compared to individual nanorods. However, the application of a nanolattice in TERS experiments can yield counterintuitive outcomes, such as uniform hotspots distributed over the nanorods instead of being localized at the ends, considering the tiny scale of the entire structure. The size of the tip–lattice assumes an important role in these

measurements; for instance, the enhancement is more pronounced when the gap size is 0.3 nm. Conversely, when the gap exceeds 0.7 nm, the lattice plasmon mode's contribution diminishes substantially, reverting to the nanorod plasmon mode.

It is important to note that in the simulation, a 20 nm tip size is employed, preventing it from reaching between the two nanorods, resulting in a dark area at the middle—similar to a scenario that may occur in the actual experiment. However, it is essential to recognize that a real tip is not a flawless, solid nanoparticle. The tip surface exhibits roughness, and its shape is irregular. Even when positioned at the midpoint of the nanorods, the tip can still make contact with the nanorod surface and effectively generate TERS signals.

CONCLUSION

This paper presents a demonstration of the distinctive electric field hotspot distribution in an Au nanorod lattice compared to that in a single nanorod. Through simulations, we reveal that the hotspot is not solely governed by the surface plasmon mode of either the individual nanorod or the lattice but is significantly influenced by the tip–lattice nanocavity. The size of this cavity becomes a crucial factor, impacting both the strength and distribution of the hotspots. These findings offer insights into the role of the nanorod lattice in gap-mode TERS experiments and provide guidance on optimizing the tip–lattice distance for effective sensing of pNTP molecules. Armed with this knowledge, the Au nanorod lattice can be more strategically employed in single-molecule imaging and photocatalysis applications using TERS.

SUPPLEMENTARY MATERIAL

See the supplementary material for (1) the experimental section including sample preparation and TERS measurement and (2) the SEM image, absorption spectrum of Au nanorods, and TERS simulations of the dual-nanorod lattice in various configurations.

ACKNOWLEDGMENTS

The work was supported by the National Natural Science Foundation of China (NNSFC) (Grant No. 22204018), the Start-up Research Fund of Southeast University (Grant No. RF1028623008), the Taishan Scholars Program (No. tsqn202306316), and the Start-up Research Fund of Shandong Institute of Advanced Technology (Grant No. 2023106R02).

AUTHOR DECLARATIONS

Conflict of Interest

The authors have no conflicts to disclose.

Author Contributions

Zhe He: Conceptualization (equal); Data curation (equal); Formal analysis (equal); Funding acquisition (equal); Investigation (equal); Methodology (equal); Visualization (equal); Writing – original draft (equal); Writing – review & editing (equal). **Jue Wang:** Formal analysis (equal); Visualization (equal); Writing – review & editing (equal). **Rui Wang:** Conceptualization (equal); Data curation (equal); Formal analysis (equal); Funding acquisition (equal); Investigation (equal); Methodology (equal); Validation (equal); Visualization (equal); Writing – original draft (equal); Writing – review & editing (equal). **Dmitry Kurouski:** Conceptualization (equal); Project administration (equal); Resources (equal); Supervision (equal); Validation (equal); Writing – review & editing (equal).

DATA AVAILABILITY

The data that support the findings of this study are available from the corresponding author upon reasonable request.

REFERENCES

[1]C. J. Murphy *et al.*, "Chemical sensing and imaging with metallic nanorods," Chem. Commun. **5**, 544–557 (2008).
[2]H. Chen, L. Shao, Q. Li, and J. Wang, "Gold nanorods and their plasmonic properties," Chem. Soc. Rev. **42**, 2679–2724 (2013).
[3]J. Zheng *et al.*, "Gold nanorods: The most versatile plasmonic nanoparticles," Chem. Rev. **121**, 13342–13453 (2021).
[4]B. Nikoobakht and M. A. El-Sayed, "Surface-enhanced Raman scattering studies on aggregated gold nanorods," J. Phys. Chem. A **107**, 3372–3378 (2003).
[5]B. Nikoobakht, J. Wang, and M. A. El-Sayed, "Surface-enhanced Raman scattering of molecules adsorbed on gold nanorods: Off-surface plasmon resonance condition," Chem. Phys. Lett. **366**, 17–23 (2002).
[6]S. Pal, A. Dutta, M. Paul, and A. Chattopadhyay, "Plasmon-enhanced chemical reaction at the hot spots of end-to-end assembled gold nanorods," J. Phys. Chem. C **124**, acs.jpcc.9b08523 (2020).
[7]H. Shen, X. Zhou, N. Zou, and P. Chen, "Single-molecule kinetics reveals a hidden surface reaction intermediate in single-nanoparticle catalysis," J. Phys. Chem. C **118**, 26902–26911 (2014).
[8]D. P. Lyvers, J.-M. Moon, A. V. Kildishev, V. M. Shalaev, and A. Wei, "Gold nanorod arrays as plasmonic cavity resonators," ACS Nano **2**, 2569–2576 (2008).
[9]S. A. Majetich, T. Wen, and R. A. Booth, "Functional magnetic nanoparticle assemblies: Formation, collective behavior, and future directions," ACS Nano **5**, 6081–6084 (2011).
[10]L. Vigderman, B. P. Khanal, and E. R. Zubarev, "Functional gold nanorods: Synthesis, self-assembly, and sensing applications," Adv. Mater. **24**, 4811–4841 (2012).
[11]S. F. Tan, U. Anand, and U. Mirsaidov, "Interactions and attachment pathways between functionalized gold nanorods," ACS Nano **11**, 1633–1640 (2017).
[12]Y. Huang and D.-H. Kim, "Dark-field microscopy studies of polarization-dependent plasmonic resonance of single gold nanorods: Rainbow nanoparticles," Nanoscale **3**, 3228–3232 (2011).
[13]J. J. Liu *et al.*, "The accurate imaging of collective gold nanorods with a polarization-dependent dark-field light scattering microscope," Anal. Chem. **95**(2), 1169–1175 (2022).
[14]S. G. Stanciu *et al.*, "Characterization of nanomaterials by locally determining their complex permittivity with scattering-type scanning near-field optical microscopy," ACS Appl. Nano Mater. **3**, 1250–1262 (2020).
[15]D. DeJarnette and D. K. Roper, "Electron energy loss spectroscopy of gold nanoparticles on graphene," J. Appl. Phys. **116**, 054313 (2014).
[16]G. T. Forcherio, D. DeJarnette, M. Benamara, and D. K. Roper, "Electron energy loss spectroscopy of surface plasmon resonances on aberrant gold nanostructures," J. Phys. Chem. C **120**, 24950–24956 (2016).
[17]X. Huang, S. Neretina, and M. A. El-Sayed, "Gold nanorods: From synthesis and properties to biological and biomedical applications," Adv. Mater. **21**, 4880–4910 (2009).
[18]A. Bhattarai, B. T. O'Callahan, C.-F. Wang, S. Wang, and P. Z. El-Khoury, "Spatio-spectral characterization of multipolar plasmonic modes of Au nanorods via tip-enhanced Raman scattering," J. Phys. Chem. Lett. **11**, 2870–2874 (2020).

[19]Z. Cao *et al.*, "Nano-gap between a gold tip and nanorod for polarization dependent surface enhanced Raman scattering," Appl. Phys. Lett. **109**, 233103 (2016).
[20]R. Wang, Z. He, and D. Kurouski, "Near-field and photocatalytic properties of mono- and bimetallic nanostructures monitored by nanocavity surface-enhanced Raman scattering," Nano Res. **16**, 1545–1551 (2023).
[21]A. M. Funston, C. Novo, T. J. Davis, and P. Mulvaney, "Plasmon coupling of gold nanorods at short distances and in different geometries," Nano Lett. **9**, 1651–1658 (2009).
[22]F. Schuknecht, K. Kołątaj, M. Steinberger, T. Liedl, and T. Lohmueller, "Accessible hotspots for single-protein SERS in DNA-origami assembled gold nanorod dimers with tip-to-tip alignment," Nat. Commun. **14**, 7192 (2023).
[23]B. Peng *et al.*, "Vertically aligned gold nanorod monolayer on arbitrary substrates: Self-assembly and femtomolar detection of food contaminants," ACS Nano **7**, 5993–6000 (2013).
[24]U. Hohenester, "Making simulations with the MNPBEM toolbox big: Hierarchical matrices and iterative solvers," Comput. Phys. Commun. **222**, 209–228 (2018).